Available online at www.sciencedirect.com
SCIENCE DIRECT®
Bioorganic & Medicinal Chemistry
ELSEVIER
Bioorganic & Medicinal Chemistry 12 (2004) 1325–1336

Outer surface modification of synthetic multifunctional pores

Pinaki Talukdar,[a] Naomi Sakai,[a] Nathalie Sordé,[a] David Gerard,[a] Valérie M. F. Cardona[b] and Stefan Matile[a,*]

[a]*Department of Organic Chemistry, University of Geneva, CH-1211 Geneva 4, Switzerland*
[b]*Department of Medical Biochemistry, University Medical Center, CH-1211 Geneva 4, Switzerland*

Received 19 December 2002; revised 9 June 2003; accepted 10 June 2003

Abstract—The characteristics of pores formed by *p*-octiphenyl β-barrels with LWV triads at the outer surface are reported in comparison with the conventional rigid-rod β-barrels with all-L outer surface. Maintained multifunctionality of tetrameric pores with external LWV triads (inversion of ion selectivity, molecular recognition and transformation) is implicative for intact barrel interior. Increased pore activity supports dominance of high bilayer affinity for W over low affinity for V. Transmembrane *p*-octiphenyl orientation (from fluorescence depth quenching) supports barrel-stave (rather than toroidal) pores and dominance of transmembrane preference of rigid rods over interfacial preference of W. Destabilization of β-barrel pores in membranes (from short single-channel lifetimes) and in the media (from 4th-power dependence on monomer concentration) by LWV triads supports dominance of low β-propensity for W over high β-propensity for V. The relation between the stability of supramolecular (pre)pores and dependence of activity on monomer concentration is discussed in a more general context.

1. Introduction

Rigid-rod β-barrel ion channels/pores **1^2–6^4** are synthetic barrel-stave supramolecules conceived to exploit the functional plasticity of their biological counterparts in bioorganic chemistry and beyond (Fig. 1).[1–3] Rigid-rod β-barrels are constructed from preorganizing *p*-octiphenyl 'staves'. Their length is adjusted to roughly match the thickness of bilayer membranes composed of egg yolk phosphatidylcholine (EYPC), their blue fluorescence is crucial for structural studies in bilayer membranes (see below). Short peptide strands are attached to each arene module of the rigid-rod molecule. Interdigitation of lateral peptides from neighboring staves yields short, eight-stranded, antiparallel β-sheets that connect these adjacent *p*-octiphenyl rods intermolecularly. Cylindrical β-sheet assembly (rather than the linear assembly) into a β-barrel is directed by seven non-planar arene-arene torsions along one *p*-octiphenyl stave. Limited internal space at the resulting *p*-octiphenyl 'turns' guides the first (Fig. 1, *B*) and the last amino-acid residue (*F* for β_5-barrels **4^4–6^4**, *D* for β_3-barrels **2^6–3^4**) to the outer barrel surface. β-Sheet conformation positions the subsequent amino-acid residues (*C* and *E* for **4^4–6^4**, *C* for **2^6–3^4**) at the inner and, with β_5-barrels **4^4–6^4**, residue *D* again at the outer barrel surface.

The possibility to install various functional groups along the ion-conducting pathway is one of the key contributions of *p*-octiphenyl β-barrels to the field of synthetic ion channels/pores.[4–19] This easy access to tunable multifunctional pores is hoped to promote the shift of attention in the field from biomimicry toward practice. With the general objective to couple molecular translocation across with molecular recognition and transformation within synthetic multifunctional pores, *p*-octiphenyl β-barrels **2^6–6^4** with internal lysine (K),[20–24] aspartate (D),[24–27] histidine (H),[24,28–34] and arginine (R)[27,33,34] residues were prepared after an initial proof of principle with 'mini-barrel' **1^2** (Fig. 1).[35]

In contrast to the internal pore design realized with rigid-rod β-barrels **2^6–6^4**, no outer surface modifications have been attempted so far (Fig. 1). These external residues in *p*-octiphenyl β-barrel ion channels, however, are expected to govern partitioning into the membrane and hydrophobic interactions with the bilayer core as well as influence β-barrel stability. Contributions of isolate amino-acid residues to partitioning have been quantified in the Wimley–White (WW) hydrophobicity scale (Table 1).[36] Clearly, the WW scale suggests that

* Corresponding author. Fax: +41-22-379-3215; e-mail: stefan.matile@unige.ch

0968-0896/$ - see front matter © 2003 Elsevier Ltd. All rights reserved.
doi:10.1016/j.bmc.2003.06.002

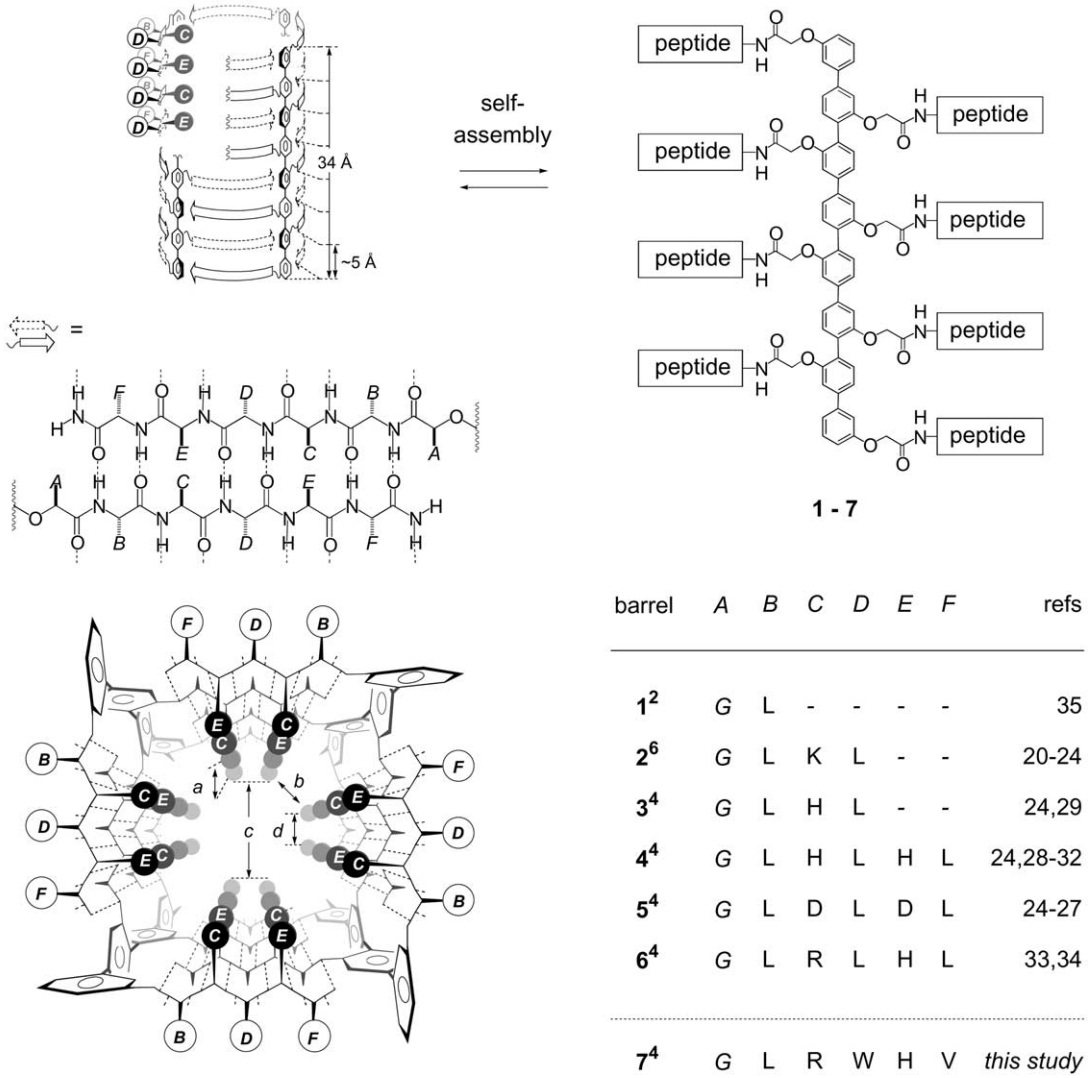

Figure 1. Self-assembly of monomeric rods **4**–**7** into *p*-octiphenyl β_5-barrels $\mathbf{4^4}$–$\mathbf{7^4}$ (analogue for **1**–**3**, not shown; expected or confirmed average aggregation numbers are indicated as superscripts; compare eq 1. Tetramers $\mathbf{4^4}$–$\mathbf{7^4}$ are given as schematic cutaway suprastructures (top) and axial views (bottom) with distances and absolute stereochemistry as in molecular models ($a \sim 5$ Å, $b \sim 4$ Å, $c \sim 14$ Å, and $d \sim 7$ Å), β-strands as arrows (top) or solid (backbone) and dotted lines (hydrogen bonds, bottom). Peptide sequences *ABCDEF*—depicted dark on white for external and white on dark for internal residues—are specified separately using single-letter abbreviations ($G = Gla = -OCH_2CO-$, bottom right). As in previous reports, we reiterate that the depicted suprastructures may be considered as, at worst, productive working hypothesis compatible with all experimental data available today.

Table 1. Selected design parameters for outer surface modifications

aa[a]	ΔG (bilayer to water, kcal/mol)[b]	β-Propensity (antiparallel)[c]
V	−0.07	2.63
I	0.31	2.60
L	0.56	1.42
F	1.13	1.23
W	1.85	0.89

[a] Amino acids (single-letter abbreviations).
[b] From ref 36.
[c] From ref 37.

replacement of the external leucines (L) in barrels $\mathbf{1^2}$–$\mathbf{6^4}$ by phenylalanines (F) and particularly tryptophans (W) should improve partitioning and consequently the activity of synthetic pores.

The propensities for antiparallel β-sheets,[37] however, suggested that external L-W and L-F mutations could destabilize the β-sheets in *p*-octiphenyl β-barrel ion channels, whereas introduction of the β-branched valine (V) or isoleucine (I) could improve β-barrel stability but reduce bilayer affinity (Table 1). To test the importance of these opposing trends, we decided to place the extreme valines (excellent β-propensity, poor partitioning) and tryptophans (poor β-propensity, excellent partitioning) at the outer surface of the same barrel-stave supramolecule, that is to make and study putative β-barrel $\mathbf{7^4}$ with external LWV triads (Fig. 1). The design of β-barrel $\mathbf{7^4}$ with external LWV triads moreover offered the opportunity to probe the transmembrane (TM) preference of rigid-rod molecules—crucial for refined architecture in matching bilayer membranes[1–3]—in competition with the interfacial (IF) preference of

tryptophan.[38–40] Internal RH dyads were chosen for **7**^{4} because homologue **6**^{4} forms ohmic ion channels with excellent stability (single-channel lifetime >20 s), invertable anion/cation selectivity at pH≈5, and superb multifunctionality with regard to internal molecular recognition and catalysis.[33,34,41]

Here, we report that the introduction of LWV triads at the outer surface of rigid-rod β-barrels results in (1) tetrameric, (2) mainly transmembrane barrel-stave pores of (3) poor stability, (4) high activity, and (5) maintained multifunctionality. These five key characteristics suggest that, within the context of rigid-rod β-barrels, TM preference of matching rods overrules IF preference of W, whereas high bilayer affinity and poor β-propensity of W and not the opposite characteristics of V govern partitioning and β-barrel stability. The multifunctional pores obtained by outer surface modification exhibit hopeless characteristics with regard to applications toward single-molecule experiments in planar bilayers,[29] whereas superb properties for practical sensing applications in spherical bilayers have already been demonstrated.[27]

2. Results and discussion

2.1. Synthesis

$1^3,2^3,3^2,4^3,5^2,6^3,7^2,8^3$-Octakis(*Gla*-Leu-Arg-Trp-His-Val-NH_2)-*p*-octiphenyl **7** was synthesized from previously reported *p*-octiphenyl **7a**[28] and commercial amino acid derivatives following the protocol used for the synthesis of $1^3,2^3,3^2,4^3,5^2,6^3,7^2,8^3$-octakis(*Gla*-Leu-Arg-Leu-His-Leu-NH_2)-*p*-octiphenyl **6** and other sequences (Scheme 1).[28,33] In brief, conventional solution-phase peptide synthesis gave pentapeptide **7b**, which was coupled with octaacid **7a**. Treatment of the product **7c** with TFA provided monomer **7** as a TFA salt. Pore characteristics discussed below suggested that monomer **7** (or self-assembled **7**^{4}) spontaneously exchanged the TFA counteranion with traces of inorganic phosphates in the environment. Validity of this interpretation, indicative for unexpectedly strong phosphate binding by oligorarginine **7**, has been supported by the presence of up to six phosphates in the ESI-MS of homologuos oligorarginine **6**;[34] oligorarginine **7** was not detectable by ESI-MS. ^{1}H NMR, MALDI-TOF-MS, and RP-HPLC supported the expected structure and sample homogeneity (see Experimental).

2.2. Multichannel characteristics in planar bilayers

The activity of putative rigid-rod β-barrel **7**^{4} in planar (black) lipid bilayers (BLMs) formed by egg yolk phosphatidylcholine (EYPC) was studied by conventional conductance experiments[42] under conditions used for the L-rich homologue **6**^{4}.[34] The multichannel characteristics of ohmic pores formed by **6**^{4} with external leucines and **7**^{4} with external LWV triads were practically identical. Most importantly, inversion of cation selective pores above pH≈5.1 to anion selective pores below pH≈5.1 (Fig. 2a) and partial blockage of anion

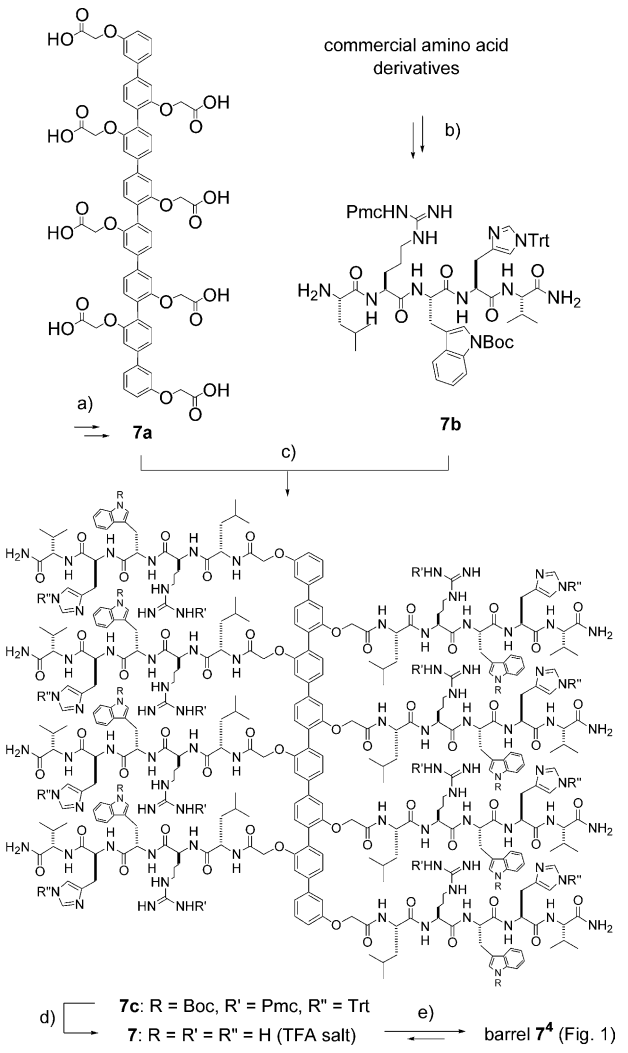

Scheme 1. (a) In nine steps from commercial biphenyl as reported;[28] (b) eight steps, see Experimental; (c) HBTU, 56%; (d) TFA, 53%; (e) self-assembly in bilayer membranes (see text).

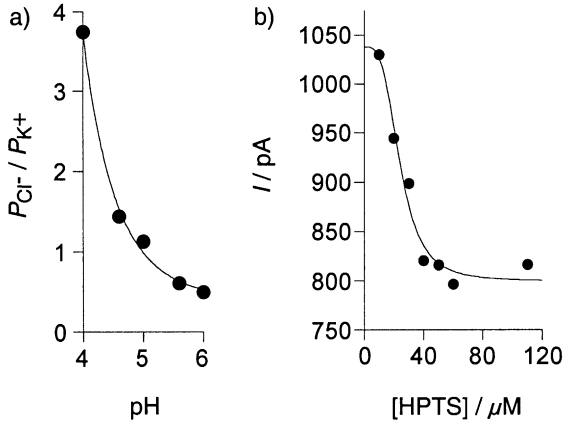

Figure 2. Macroscopic currents of pore **7**^{4} (30 nM *cis*) in EYPC BLMs: (a) ion selectivity in asymmetric KCl (1.0 M *cis*, 100 mM *trans*) as a function of pH (permeability ratios determined from *I*–*V* curves using GHK eq); (b) macroscopic current of **7**^{4} (30 nM *cis*) as a function of HPTS concentration (*trans*) at pH = 4.6 with curve fit to Hill equation ($V = +50$ mV, $K_D = 24.1 \pm 3.1$ μM, $n = 3.4 \pm 1.4$).

selective pores at pH <5.1 with HPTS ($K_D \approx 30$ μM at $+50$ mV and pH 4.6, Fig. 2b) were not affected by outer surface modification.[34] Preliminary results indicated that—in excellent agreement with the proposed structures and mechanisms—the esterolytic activity of H-rich rigid-rod β-barrel **4**[4] is little influenced by the introduction of internal RH dyads in **6**[4] and **7**[4] as well as external LWV triads in **7**[4].[28–30,34,41]

About intact multifunctionality of rigid-rod β-barrel **7**[4] with external LWV triads suggested that at least part of the suprastructural characteristics determined for rigid-rod β-barrel **6**[4] are maintained as well. For instance, maintained selectivity inversion confirmed presence of internal guanidinium-phosphate complexes and, as evidenced by HPTS blockage, internal molecular recognition by anion exchange applies also for barrel **7**[4].[34] Only ~25%-blockage of pores **7**[4] by HPTS (compared to >50%-blockage of **6**[4]) was, however, consistent with contributions from less ordered 'pro-β-barrel' suprastructures (see below).

2.3. Single-channel characteristics

Rigid-rod β-barrel **6**[4] with external leucines formed single channels of superb stability ($\tau > 20$ s).[34] Under identical conditions, putative rigid-rod β-barrel **7**[4] with external LWV triads exhibited strikingly different, short-lived bursts reminiscent of pores formed by α-helical peptides (i.e., 'α-barrels')[43–45] and *p*-octiphenyl push-pull 'α_{lk}-barrels' (Fig. 3a).[23] Longer-lived open conductances of irregular magnitude could be detected occasionally (Fig. 3b). Because of their rare occurrence, however, we felt that interpretation with regard to homogeneity, lifetimes, and diameters[23,29] was not meaningful in this case. The roughly intact multifunctionality of **7**[4] (above and refs 27 and 41), however, suggested that either the population of long-lived ion channels is higher than expected under certain conditions or that some aspects of multifunctionality do not require stable ion channels (see below).

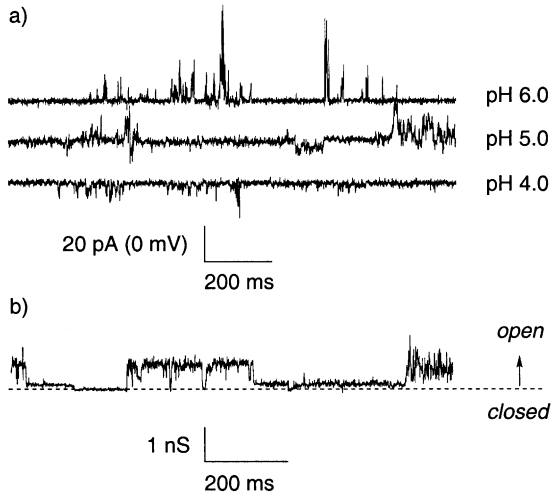

Figure 3. Single-channel recordings of pore **7**[4] (30 nM *cis*) in EYPC BLMs at (a) 0 mV in asymmetric KCl (1.0 M *cis*, 100 mM *trans*) at pH = 6.0 (top), pH = 5.0 (middle), pH = 4.0 (bottom) and (b) +50 mV in symmetric KCl (1.0 M) at pH = 6.0.

To elaborate on the latter possibility, ion selectivity of pore **7**[4] was also tested on the single-molecule level. Without applied voltage (i.e., $V = 0$ mV), short-lived bursts of positive sign corresponding to reversal potentials $V_r < 0$ mV confirmed the expected cation selectivity at pH = 6.0 (Fig. 3a, top). Compatible with anion selectivity, bursts of negative sign corresponding to $V_r > 0$ mV were detected at pH = 4.0 (Fig. 3a, bottom). At pH = 5.0, near selectivity inversion, however, short-lived bursts of both positive and negative signs were recorded (Fig. 3a, middle). This indicated that the macroscopic disappearance of ion selectivity around pH≈5.0 is caused by a 1:1 mixture of anion and cation selective pores **7**[4]. It further demonstrated that inversion of anion/cation selectivity at pH≈5 is possible with short-lived pores.

2.4. Fluorescence depth quenching in spherical bilayers

The most straightforward explanation for the short-lived bursts seen in single-channel experiments was that W-enforced interfacial (IF) location of W-rich *p*-octiphenyl **7** induces defects in the lipid packing.[38–40,43–45] To test this hypothesis, location and orientation of the blue-emitting *p*-octiphenyls **7** were determined in EYPC LUVs by fluorescence depth quenching method (FDQ). Simple, sensitive, and non-invasive FDQ is possible with fluorescent rods using two spin-labeled EYPC LUVs, one with central (CR) 12-DOXYL-quenchers near the middle of the bilayer and the other one with IF 5-DOXYL-quenchers.[2,21–23,46,47] Comparison of the efficiency of CR and IF quenchers with the *p*-octiphenyl emission in unlabeled EYPC LUVs allows to differentiate between CR, IF, and TM rod orientation as outlined in Figure 4a.

At pH = 7.0, the ability of CR (dotted) and IF quencher (solid) to reduce the emission intensity of *p*-octiphenyl **7** in unlabeled EYPC LUVs (bold) was about the same (Fig. 4b). At pH = 4.0, the quenching efficiency of CR (dotted) exceeded that of IF quencher (solid) slightly (Fig. 4c). These FDQ results demonstrated absence of the anticipated IF preference driven by tryptophans. IF location was observed previously with truncated *p*-sexiphenyls[47] and with *p*-octiphenyl β-barrels in highly polarized bilayers.[23] The situation at pH = 7 was apparently dominated by the preferred TM orientation of rigid-rod molecules in hydrophobically matching lipid bilayers. Charge repulsion between the protonated histidines of rods in the membrane and rods in the media may then account for an increased CR population contributing to the situation at pH = 4.0. This high concentration (high protonation) effect has been observed previously by us[23] and others;[48] functional relevance of small CR populations at low pH is unlikely (compare Fig. 3a and ref 34).

Clear absence of appreciable IF populations at pH = 7.0 and pH = 4.0 was of importance beyond the comparison of competing IF preference of W and TM preference of rods. It further ruled out pore formation mechanisms operating by disruption of the bilayer packing from the interface as in 'toroidal pores' or in 'carpet mechanisms' often found with α-helix bundles.[43–45]

2.5. pH Profiles in spherical bilayers

The pH dependence of pore formation by rigid-rod β-barrels **6**^{4} and **7**^{4} was determined with the ANTS/DPX assay used previously to obtain pH profiles for tetramers **3**^{4}–**5**^{4} and hexamer **2**^{6}.[24] In brief, large unilamellar vesicles (LUVs) composed of EYPC were loaded with fluorophore ANTS and quencher DPX. In this nearly pH independent assay, pore formation is followed by an increase in ANTS emission due to efflux of anion ANTS and/or cation DPX.

The pH profiles of rigid-rod β-barrels **6**^{4} (filled squares) and **7**^{4} (filled circles) with internal RH dyads were overall similar to those obtained for rigid-rod β-barrels **3**^{4} (empty circles) and **4**^{4} (empty squares) with internal histidines only (Fig. 5). The latter profiles were previously rationalized with the internal charge repulsion (ICR) model (i.e., the general requirement of intermediate ICR for high open probability of supramolecular pores), imposing partial protonation of internal histidines as essential for function of pores **3**^{4}/**4**^{4} at (3.5 <) pH < 5.5.[24] The overall surprisingly weak influence of internal arginines in rigid-rod β-barrels **6**^{4}/**7**^{4} (filled symbols) on the pH profile compared to that of all-H **3**^{4}/**4**^{4} (empty symbols) was consistent with little *ICR* contributions due to the weak electrostatic interaction well known with guanidinium cations.[24,34,49]

The relatively small increase in activity of **6**^{4} at pH < ~6.5 could be due to hindered ANTS efflux through the very stable channel filled with strongly bound counter anions (e.g., inorganic phosphates)[34] compared to 'free' efflux through the 'empty,' less stable ion channel **4**^{4}.[28] Poor partitioning due to competing fibrillogenesis from the stabilized aqueous prepores[32] may be envisioned alternatively to rationalize this phenomenon (see below). Instability of the barrel with external LWV triads and thus more hindered fibrillogenesis in solution, improved partitioning (Table 1), and less hindered ANTS/DPX efflux through less ordered pores may then similarly contribute to the larger increase in activity at slightly higher pH < 7 with rigid-rod β-barrel **7**^{4}. More complex and interconnected contributions from several additional parameters to the pH profiles of H(R)-rich pores can, however, not be excluded. Moreover, discussion of these small differences should not distract from the fact that — consistent with the *ICR* model[24] — the pH profiles of H(R)-rich rigid-rod β-barrels **3**^{4}, **4**^{4}, **6**^{4} and **7**^{4} are overall very similar when compared to D-rich **5**^{4} or K-rich **2**^{6}.[24]

2.6. Concentration dependence in spherical bilayers

The dependence of the fractional activity Y up to 0.5 on the concentration of monomeric rods **6** and **7** (i.e., $c_{M,Y<0.5}$) was determined with the ANTS/DPX assay. The activity of pore **6**^{4} exhibited 'premature saturation' at $Y < 0.5$ (Fig. 6, filled squares). The activity of pore **7**^{4}, in contrast, showed about fourth-power dependence on monomer concentration (Fig. 6, filled circles). Linear concentration dependence of H-rich rigid-rod β-barrels **3**^{4} and **4**^{4} has been reported previously (Fig. 6, empty symbols).[24]

The three distinct $c_{M,Y<0.5}$ profiles of rigid-rod β-barrels **3**^{4}/**4**^{4}, **6**^{4} and **7**^{4} provided a marvelous illustration for the concise expression of pore formation mechanisms in $c_{M,Y<0.5}$ profiles. Excluding contributions from pore blockers (well described with, e.g., the Hill equation),[25–27] the fractional activity Y of supramolecular pores depends on monomer concentration c_M and voltage V in the following manner

$$Y \propto c_M{}^n \exp(z_g eV/kT) \quad (1)^{23}$$

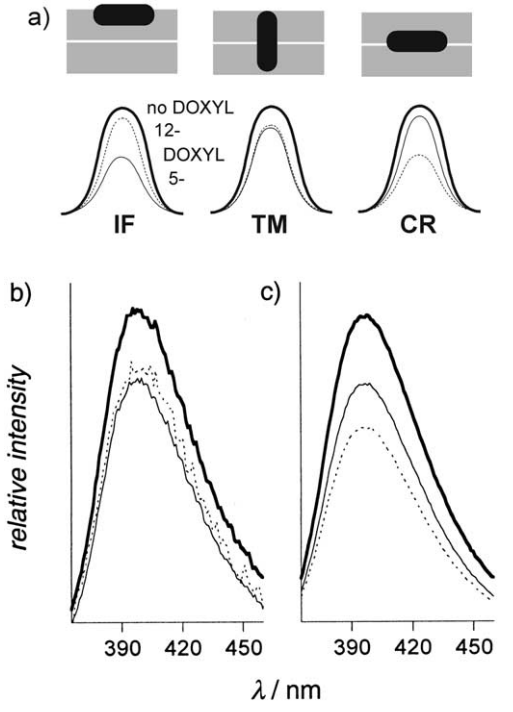

Figure 4. Fluorescence depth quenching (FDQ) of fluorescent rod **7** (c_M = 200 nM, λ_{ex} = 320 nm) in EYPC LUVs without (bold) and with IF (10% 5-DOXYL-PC, solid) or CR quencher (10% 12-DOXYL-PC, dotted) at pH = 7.0 (b) and pH = 4.0 (c). (a) Schematic representation of FDQ results indicating interfacial (IF), transmembrane (TM), and central (CR) *p*-octiphenyl rods (black) in EYPC bilayers (gray).

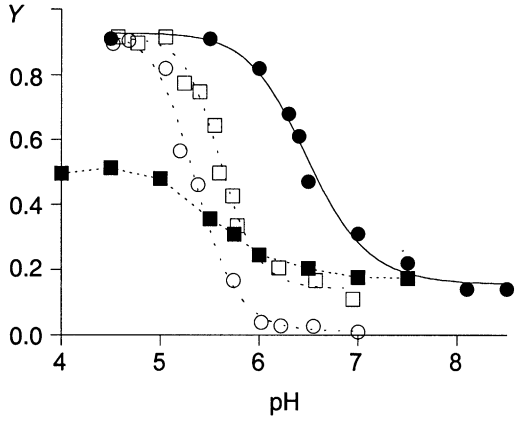

Figure 5. pH Profile of pore **7**^{4} (c_M = 100 nM) in EYPC LUVs (filled circles) in comparison to pore **6**^{4} (c_M = 160 nM, filled squares), pore **4**^{4} (empty squares) and pore **3**^{4} (empty circles) determined using the ANTS/DPX assay; data for **3**^{4}/**4**^{4} taken from ref 24.

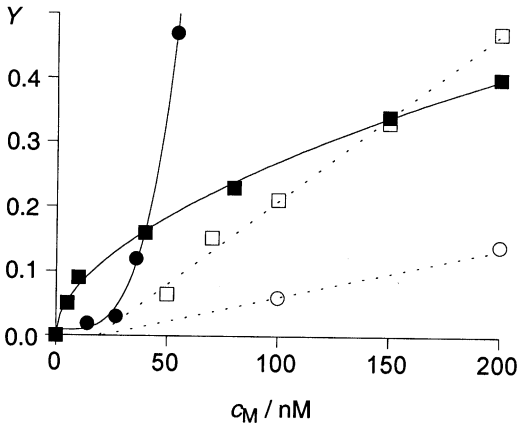

Figure 6. $c_{M,Y<0.5}$ Profile of pore **7**^{4} in EYPC LUVs (filled circles, at pH = 5.5) in comparison to pore **6**^{4} (filled squares, at pH = 4.5), pore **4**^{4} (empty squares) and pore **3**^{4} (empty circles) using the ANTS/DPX assay; data for **4**^{4}/**3**^{4} taken from ref 24.

Non-linear $c_{M,Y<0.5}$ profiles with $n>1$ provide the average number of monomers self-assembled in an active pore. This situation was also found for pores **7**^{4} with $n=3.7\pm0.6$, formed, therefore, by in average about four *p*-octiphenyl staves (Fig. 6, filled circles). Similar behavior was reported previously for K-rich hexamers comprising eight-stranded β-sheets (i.e., **2**^{6})[21] and K-rich tetramers with six-stranded β-sheets.[20,24] Given some counterproductive controversies in the field with regard to structure determination of synthetic ion channels/pores, it may be important to reiterate that $n>1$ behavior demonstrates that the dissociation constant (K_D) of the active pore is far above $c_{M,Y<0.5}$. This implies that application of conventional methods to determine the active structure of $n>1$ pores like **7**^{4} is meaningless, potentially erroneous, and, at worst, misleading.

Linear $c_{M,Y<0.5}$ profiles with $n\approx1$ can indicate monomeric pores, particularly if $c_{M,Y=0}=0$ nM. Alternatively, $n\approx1$ can originate from incompatibility with the assumption $K_D \gg c_{M,Y<0.5}$ underlying eq 1, that is indicate $K_D \leq c_{M,Y<0.5}$ for both active supramolecular pores in the bilayer and prepores in the media. This situation could result in $c_{M,Y=0}>0$ nM. With various lines of evidence in favor of mainly tetrameric rigid-rod β-barrels in hand,[24,28–32] $c_{M,Y=0}\approx20$ nM therefore supported presence of (pre)pores **3**^{4}/**4**^{4} with low nanomolar K_D. A clearly biphasic mechanism with $n\approx4$ at low $c_{M,Y<0.3}$ and $n\approx1$ at high $c_{M,Y>0.3}$ was reported previously for tetramers **5**^{4}.[25]

The third possibility, that is a non-linear $c_{M,Y<0.5}$ profile with $n<1$, was observed for pores **6**^{4} ($n=0.6\pm0.03$, Fig. 6, filled squares). Without doubt, interpretation in terms of eq. 1 is meaningless in this case. The $n<1$ behavior may be understood as extreme expression of above situation with $n\approx1$ for highly exothermic (pre)pore formation (i.e., $K_D \ll c_{M,Y<0.5}$ instead of $K_D \leq c_{M,Y<0.5}$ with $n\approx1$). Namely, with $K_D \ll c_{M,Y<0.5}$, 'premature saturation' at $c_{M,Y<0.5}$ is conceivable as indicative for increasing fibrillogenesis with increasing concentration of highly stable prepores, thereby reducing the effective prepore concentration in solution as well as bilayer. A critical fibril concentration of $c_M=3$ μM (i.e., clearly above $c_{M,Y=0.5}=0.2$ μM) has been determined previously for β-fibrillogenesis from aqueous prepores **4**^{4} ($n\approx1$);[32] $n<1$ suggested that the critical fibril concentration of **6**^{4} is well below this value.

In summary, above interpretation suggested that, at least for the *p*-octiphenyl β $_5$-barrels on hand, the dissociation constants of the corresponding (pre)pores can be qualitatively deduced from c_M profiles. The identified order, that is **6**^{4} ($n<1$: $K_D \ll c_{M,Y<0.5}$) > **4**^{4} ($n\approx1$: $K_D \leq c_{M,Y<0.5}$) ≥ **5**^{4} ($n\geq1$: $K_D \leq c_{M,Y<0.5}$) > **7**^{4} ($n>1$: $K_D \gg c_{M,Y<0.5}$), is in good agreement with various lines of experimental evidence including single-channel lifetimes (**6**^{4} ≫ **4**^{4} ≈ **5**^{4} > **7**^{4}).[28,34] Despite this satisfactory situation, it is important to caution that, as with pH profiles, the origin of $c_{M,Y<0.5}$ profiles of synthetic multifunctional pores is, presumably, more complex than it may appear in above discussion. Considering alternative parameters that may influence rate-limiting steps in pore formation, it is important to avoid overgeneralization of above interpretation of c_M profiles. For example, all pores formed by β_3-barrels exhibited superb stability, independent of $n\approx1$ as with tetramer **3**^{4} or $n>1$ as with hexamer **2**^{6}.[21,22,29]

2.7. Putative mechanisms of action

Although speculations on the suprastructural and mechanistic origins of function in complex systems need much caution, we consider careful elaboration of speculative working hypotheses based on experimental evidence an important effort to summarize results and stimulate future progress in the field. In this spirit, we recapitulate that (a) injection of monomeric rods **4** into the media results in (b) self-assembly of aqueous monomers (**AQ**^{1}) into aqueous prepores (β-**AQ**^{4}) with β_5-barrel suprastructure similar to that of the active pore β-**TM**^{4} (Fig. 7A).[28–32] At elevated concentrations ($c_M>3$ μM),[32] fibrillogenesis to give insoluble β-**F**^{n} (c) competes with partitioning of prepore β-**AQ**^{4} to give active pore β-**TM**^{4} (d).[32] Rigid-rod β_5-barrels **5**^{4} and **6**^{4} with modified inner but unchanged outer surface seem to follow essentially the same mechanism.[25,26,34] Consequences of inner surface modification on the stability of β-**TM**^{4} (and thus β-**AQ**^{4}) expressed in single-channel lifetimes (**6**^{4} ≫ **4**^{4} ≈ **5**^{4})[28,34] as well as biphasic ($n\geq1$; **5**^{4})[25] and crooked c_M profiles ($n<1$; **6**^{4}, Fig. 6) are compatible with increased populations of **AQ**^{1} (for **5**^{4}) and β-**F**^{n} (for **6**^{4}).

Outer surface modification from all-L pores **4**^{4}–**6**^{4} to pore **7**^{4} with LWV triads had as little influence on the multifunctionality of the barrel interior as expected (Fig. 2). The impact of outer surface modifications on barrel stability was, however, sufficient to impose an alternative pore formation mechanism (Fig. 7B). Namely, low β-propensity of W seems to hinder self-assembly of **AQ**^{1} into (b) prepore β-**AQ**^{4}, (d) pore β-**TM**^{4}, and fibrils β-**F**^{n} (c, Fig. 7). High membrane-affinity of W and TM preference of rigid rods, on the other hand, support formation of active tetramers **pro**-β-**TM**^{4}

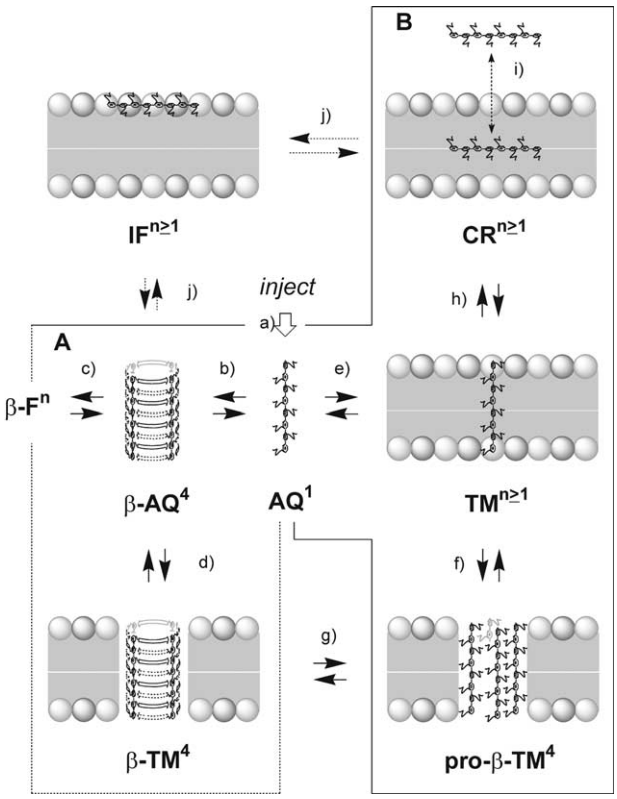

Figure 7. Putative mechanisms of action for (**A**) previous *p*-octiphenyls **3**–**6** and (**B**) novel *p*-octiphenyl **7** (simplified, see text for discussion).

from **AQ^1** (e, f), presumably via monomer/oligomer **TM$^{n\geq1}$** (e). Partial reorientation from TM toward CR (h) but not IF populations (j) to minimize repulsion from rods in the media (i) with increasing rod concentration or charge may be of little importance for function but essential to interpret eventual structural studies with less sensitive methods appropriately. Experimental support for these claims comes from a $c_{M,Y<0.5}$ profile with $n\approx4$ (implicative for $c_M > c_{oligomer}$ and for oligomers≈tetramers), FDQ (implicative for TM > CR ≫ IF), and short single-channel lifetime (implicative for **pro-β-TM^4** > **β-TM^4**).

Pores **pro-β-TM^4** found with **7^4** may thus be best described as unstable tetramers of TM *p*-octiphenyls with unknown peptide conformation (Figs 7 and 3a), that can transform—hindered by W—into more stable rigid-rod β-barrel **β-TM^4** (Figs 7 and 3b). Different to the situation with push-pull *p*-octiphenyl $\alpha_{/k}$- and β-barrels,[23] direct observation of the transition of unstable **pro-β-TM^4** to stable **β-TM^4** **7^4** was not possible on the single-molecule level.

Exclusive explanation of the found pore characteristics with either transient **pro-β-TM^4** or more stable **β-TM^4** seems difficult, in part impossible. For example, it is difficult to understand how transient **pro-β-TM^4** pores formed by oligoarginine **7** and stable **β-TM^4** pores formed by homologue **6** could share distinct characteristics like phosphate binding, inversion of anion/cation selectivity, HPTS blockage, and catalysis. A reasonably satisfactory explanation would be that pores formed by **pro-β-TM^4** and **β-TM^4** are very different in stability but very similar in structure. Moreover, template effects from counteranions like inorganic phosphate or HPTS are expected to influence the transition of **pro-β-TM^4** to **β-TM^4** (Fig. 7g) but notoriously difficult to confirm experimentally.

3. Summary and conclusions

The here reported characteristics of pores **7^4** with external LWV triads are dominated by poor stability not only of the identified, highly active pores (with TM orientation and roughly maintained multifunctionality), but also of aqueous prepores and rigid-rod β-fibrils. The experimental 'signature' of pores **7^4** compared to previous rigid-rod β-barrels **3^4**–**6^4** of comparable global structure are non-linear c_M profile in spherical and short-lived 'single-channel' bursts with occasional transition to more stable channels in planar bilayers. From a methodological point of view, the reported results and discussions may help to illustrate why structural studies on synthetic ion channels/pores are meaningful only if compatibility with pH profile, c_M profile, and related insights from function is demonstrated. With regard to practical applications, the characteristics found for pore **7^4** can be ranked from disastrous (for single-molecule chemistry within synthetic pores)[29] to superb (for fluorometric enzyme sensing).[27]

4. Experimental

4.1. Materials

As in ref 28, supporting information, with the following additions. ^{1}H and ^{13}C NMR spectra were recorded on Bruker-AV 300, 400 and 500 spectrometers at 25 °C, chemical shifts being expressed in ppm with TMS as an internal standard. IR spectra were recorded on Perkin–Elmer 1600 FT-IR spectrometer. Identity of the final product **7** was confirmed by MALDI-TOF STR DE (PE Biosystems, Foster City, CA, USA). EYPC, 5- and 12-DOXYL-PC, and Mini-Extruder were purchased from Avanti Polar Lipids (Alabaster, AL, USA), HPTS, ANTS and DPX from Molecular Probes (Eugene, OR), detergents, all salts and buffers of the best grade available from Sigma-Aldrich Corp (St. Louis, MO, USA), and used as received. Amino acid derivatives were from Novabiochem or Bachem, reagents and solvents from Acros or Fluka-Aldrich.

4.2. Fmoc-His(Trt)-Val-NH$_2$ (general procedure A)

To a solution of H-Val-NH$_2$·HCl (2.00 g, 3.23 mmol) in CH_2Cl_2 (20 mL), EDC·HCl (866 mg, 4.52 mmol), HOBt (524 mg, 3.87 mmol), Et_3N (2.58 mL, 18.4 mmol) and Fmoc-His(Trt)-OH (591 mg, 3.87 mmol) were added at 0 °C and stirred overnight at rt. The reaction mixture was diluted with CH_2Cl_2 and washed successively with 1 M aqueous $NaHSO_4$ (2×150 mL), brine (100 mL), saturated aqueous $NaHCO_3$ (2×150 mL) and brine (150

mL), dried over anhydrous Na_2SO_4 and concentrated in vacuo. Purification of the crude product by column chromatography (CH_2Cl_2/MeOH 10:1, $R_f = 0.6$; first with 25:1, then to 15:1) yielded pure Fmoc-His(Trt)-Val-NH_2 (1.72 g, 74%) as colorless solid. α_D^{20} −10.2 (*c* 1.00, MeOH); mp: 107.0–107.5 °C; IR (film) ν 3310 (m), 3016 (m), 1710 (s), 1661 (s), 1518 (m) cm^{-1}; ^1H NMR (500 MHz, CD_3OD): δ 7.76 (d, $J = 7.6$ Hz, 2H), 7.57 (d, $J = 7.3$ Hz, 2H), 7.34 (m, 2H), 7.33 (s, 1H), 7.31–7.24 (m, 9H), 7.22 (m, 2H), 7.10–7.02 (m, 6H), 6.78 (s, 1H), 4.48 (dd, $J = 9.6$, 4.6 Hz, 1H), 4.24 (d, $J = 7.1$ Hz, 2H), 4.23 (d, $J = 6.7$ Hz, 1H), 4.08 (t, $J = 7.1$ Hz, 1H), 3.05 (dd, $J = 14.8$, 4.6 Hz, 1H), 2.83 (dd, $J = 14.8$, 9.6 Hz, 1H), 2.09 (m, 1H), 0.93 (d, $J = 6.9$ Hz, 3H), 0.91 (d, $J = 6.8$ Hz, 3H); ^{13}C NMR (125 MHz, CD_3OD): δ 175.91 (s), 173.92 (s), 158.29 (s), 145.20 (s), 145.11 (s), 143.60 (s×3), 142.54 (s), 142.52 (s), 139.48 (d), 137.89 (s), 130.85 (d×6), 129.26 (d×3), 129.19 (d×6), 128.80 (d×2), 128.20 (d), 128.17 (d), 126.27 (d×2), 121.10 (d), 120.93 (d×2), 76.80 (s), 68.15 (t), 59.54 (d), 56.46 (d), 48.31 (d), 32.02 (d), 31.63 (t), 19.78 (q), 18.19 (q); anal. calcd for $C_{45}H_{43}N_5O_4$: C 75.29, H 6.04, N 9.76; found: C 72.43, H 5.96, N 9.38; MS (ESI, MeOH): *m*/*z* (%) 718 (60) $M + H^+$, 740 (100) $M + Na^+$.

4.3. H-His(Trt)-Val-NH_2 (general procedure B)

To a solution of Fmoc-His(Trt)-Val-NH_2 (1.61 g, 2.24 mmol) in DMF (10 mL), piperidine (0.2 mL) was added and stirred for 10 min at rt. Concentration in vacuo and purification of the crude product by column chromatography (CH_2Cl_2/MeOH 10:1, $R_f = 0.3$; first with 15:1, then to 6.7:1) furnished pure H-His(Trt)-Val-NH_2 (1.09 g, 98%) as a colorless solid. α_D^{20} −6.90 (*c* 1.00, MeOH); mp: 82.0–83.0 °C; IR (film) ν 3302 (m), 3177 (m), 1657 (s), 1511 (m) cm^{-1}; ^1H NMR (500 MHz, CD_3OD): δ 7.38–7.34 (m, 10H), 7.16–7.11 (m, 6H), 6.78 (s, 1H), 4.20 (d, $J = 6.0$ Hz, 1H), 3.64 (dd, $J = 7.5$, 5.0 Hz, 1H), 2.94 (dd, $J = 14.5$, 5.0 Hz, 1H), 2.74 (dd, $J = 14.5$, 7.5 Hz, 1H), 2.09 (m, 1H), 0.92 (d, $J = 6.6$ Hz, 3H), 0.90 (d, $J = 6.6$ Hz, 3H); ^{13}C NMR (125 MHz, CD_3OD): δ 176.60 (s), 176.05 (s), 143.71 (s×3), 139.79 (d), 138.19 (s), 130.88 (d×6), 129.30 (d×3), 129.25 (d×6), 121.24 (d), 76.85 (s), 59.32 (d), 56.14 (d), 34.47 (t), 31.95 (d), 19.77 (q), 18.15 (q); anal. calcd for $C_{30}H_{33}N_5O_2$: C 72.70, H 6.71, N 14.13; found: C 68.74, H 6.84, N 13.01; MS (ESI, MeOH): *m*/*z* (%) 496 (8) $M + H^+$, 518 (80) $M + Na^+$, 1014 (100) $2M + Na^+$.

4.4. Fmoc-Trp(Boc)-His(Trt)-Val-NH_2

Coupling of H-His(Trt)-Val-NH_2 (1.49 g, 3.01 mmol) with Fmoc-Trp(Boc)-OH (2.22 g, 4.21 mmol) following procedure A and purification of the crude product by column chromatography (CH_2Cl_2/MeOH 20:1 $R_f = 0.4$) yielded Fmoc-Trp(Boc)-His(Trt)-Val-NH_2 (2.11 g, 70%) as a colorless solid. α_D^{20} −9.70 (*c* 1.00, MeOH); mp: 127.0–127.5 °C; IR (film) ν 3290 (m), 3061 (m), 1724 (s), 1652 (s), 1522 (m) cm^{-1}; ^1H NMR (500 MHz, CD_3OD): δ 8.06 (br. d, $J = 7.6$ Hz, 1H), 7.70 (d, $J = 7.5$ Hz, 1H), 7.67 (d, $J = 7.5$ Hz, 1H), 7.60 (d, $J = 7.5$ Hz, 1H), 7.56 (s, 1H), 7.42 (d, $J = 7.5$ Hz, 1H), 7.41 (d, $J = 7.5$ Hz, 1H), 7.30 (m, 1H), 7.25 (s, 1H), 7.24 (m, 1H), 7.23 (m, 9H), 7.20 (m, 1H), 7.19 (m, 1H), 7.13 (t, $J = 7.5$ Hz, 1H), 7.12 (t, $J = 7.5$ Hz, 1H), 7.01 (m, 6H), 6.74 (s, 1H), 4.62 (t, $J = 6.0$ Hz, 1H), 4.47 (dd, $J = 9.8$, 4.5 Hz, 1H), 4.20 (dd, $J = 10.5$, 6.9 Hz, 1H), 4.18 (d, $J = 6.0$ Hz, 1H), 4.01 (br. t, $J = 7.3$ Hz, 1H), 3.90 (dd, $J = 10.5$, 7.6 Hz, 1H), 3.21 (dd, $J = 15.2$, 4.5 Hz, 1H), 3.03 (dd, $J = 15.2$, 9.8 Hz, 1H), 2.90 (d, $J = 6.0$ Hz, 2H), 2.09 (m, 1H), 1.54 (s, 9H), 0.87 (d, $J = 6.7$ Hz, 3H), 0.86 (d, $J = 7.0$ Hz, 3H); ^{13}C NMR (125 MHz, CD_3OD): δ 175.91 (s), 174.14 (s), 173.12 (s), 158.31 (s), 150.90 (s), 144.95 (d×2), 143.58 (s×3), 142.50 (s), 142.42 (s), 139.70 (d), 137.43 (s), 136.82 (s), 131.76 (s), 130.80 (d×6), 129.20 (d×3), 129.16 (d×6), 128.75 (d), 128.73 (d), 128.11 (d), 128.07 (d), 126.34 (d), 126.13 (d), 125.45 (d), 125.33 (d), 123.66 (d), 121.09 (d), 120.94 (d), 120.88 (d), 120.10 (d), 117.47 (s), 116.17 (d), 84.68 (s), 76.73 (s), 68.21 (t), 59.76 (d), 56.56 (d), 55.13 (d), 48.19 (d), 31.61 (d), 30.73 (t), 28.43 (t), 28.36 (q×3), 19.84 (q), 18.34 (q); anal. calcd for $C_{61}H_{61}N_7O_7$: C 72.96, H 6.12, N 9.76; found: C 70.29, H 6.03, N 9.34; MS (ESI, MeOH): *m*/*z* (%) 1004 (11) $M + H^+$, 1027 (100) $M + Na^+$.

4.5. H-Trp(Boc)-His(Trt)-Val-NH_2

Deprotection of Fmoc-Trp(Boc)-His(Trt)-Val-NH_2 (1.65 g, 1.64 mmol) following the procedure B and purification of the crude product by column chromatography (CH_2Cl_2/MeOH 10:1, $R_f = 0.3$; first with 20:1, then to 13:1) furnished pure H-Trp(Boc)-His(Trt)-Val-NH_2 (1.18 g, 92%) as a colorless solid. α_D^{20} −4.00 (*c* 1.00, MeOH); mp : 112.0–113.0 °C; IR (film) ν 3303 (m), 3045 (m), 1722 (s), 1649 (s), 1503 (m) cm^{-1}; ^1H NMR (400 MHz, CD_3OD): δ 8.05 (br. d, $J = 8.1$ Hz, 1H), 7.60 (dd, $J = 7.1$, 0.8 Hz, 1H), 7.48 (s, 1H), 7.38-7.34 (m, 1H), 7.36 (m, 9H), 7.24 (dt, $J = 7.7$, 0.8 Hz, 1H), 7.19 (dt, $J = 7.7$, 1.0 Hz, 1H), 7.10 (m, 6H), 6.65 (d, $J = 1.0$ Hz, 1H), 4.68 (dd, $J = 7.0$, 5.3 Hz, 1H), 4.22 (d, $J = 6.0$ Hz, 1H), 3.66 (dd, $J = 7.6$, 5.0 Hz, 1H), 3.09 (dd, $J = 14.4$, 5.0 Hz, 1H), 2.95 (dd, $J = 14.9$, 5.3 Hz, 1H), 2.87 (dd, $J = 14.9$, 7.0 Hz, 1H), 2.86 (dd, $J = 14.4$, 7.6 Hz, 1H), 2.14 (m, 1H), 1.66 (s, 9H), 0.94 (d, $J = 6.6$ Hz, 3H), 0.93 (d, $J = 6.8$ Hz, 3H); ^{13}C NMR (100 MHz, CD_3OD): δ 175.52 (s), 174.61 (s), 171.82 (s), 149.54 (s), 142.23 (s×3), 138.19 (d), 135.95 (s), 135.50 (s), 130.33 (s), 129.49 (d×6), 127.90 (d×3), 127.86 (d×6), 124.13 (d), 124.09 (d), 122.26 (d), 119.78 (d), 118.88 (d), 116.10 (s), 114.77 (d), 83.42 (s), 75.38 (s), 58.25 (d), 54.43 (d), 52.78 (d), 30.30 (d), 30.12 (t), 29.86 (t), 27.04 (q×3), 18.36 (q), 16.71 (q); anal. calcd for $C_{46}H_{51}N_7O_5$: C 70.66, H 6.57, N 12.54; found: C 67.45, H 6.57, N 11.68; MS (ESI, MeOH): *m*/*z* (%) 783 (40) $M + H^+$, 805 (61) $M + Na^+$, 1564 (16) $2M + H^+$, 1587 (100) $2M + Na^+$, 2368 (12) $3M + Na^+$.

4.6. *Z*-Arg(Pmc)-Trp(Boc)-His(Trt)-Val-NH_2

Coupling of H-Trp(Boc)-His(Trt)-Val-NH_2 (1.18 g, 1.51 mmol) with *Z*-Arg(Pmc)-OH (1.04 g, 1.81 mmol) following the procedure A and purification of the crude product by column chromatography (CH_2Cl_2/MeOH 10:1, $R_f = 0.5$; first with 20:1, then to 10:1) furnished pure *Z*-Arg(Pmc)-Trp(Boc)-His(Trt)-Val-NH_2 (1.88 g, 93%) as colorless solid. α_D^{20} −12.3 (*c* 1.00, MeOH); mp:

138.0–138.5 °C, IR (film) ν 3316 (m), 3055 (m), 1721 (s), 1659 (s) cm^{-1}; ^1H NMR (500 MHz, CD_3OD): δ 8.03 (br. d, $J=7.7$ Hz, 1H), 7.53 (d, $J=7.7$ Hz, 1H), 7.49 (s, 1H), 7.37 (s, 1H), 7.33–7.20 (m, 14H), 7.22 (m, 1H), 7.15 (m, 1H), 7.10–7.07 (m, 6H), 6.80 (s, 1H), 5.03 (d, $J=12.5$ Hz, 1H), 4.92 (d, $J=12.5$ Hz, 1H), 4.67–4.61 (m, 2H), 4.17 (d, $J=5.8$ Hz, 1H), 4.03 (dd, $J=7.3$, 6.2 Hz, 1H), 3.18 (dd, $J=14.5$, 4.4 Hz, 1H), 3.04–2.88 (m, 5H), 2.59 (t, $J=6.8$ Hz, 2H), 2.54 (s, 3H), 2.51 (s, 3H), 2.10–2.05 (m, 1H), 2.05 (s, 3H), 1.76 (t, $J=6.8$ Hz, 2H), 1.62–1.57 (m, 1H), 1.60 (s, 9H), 1.48 (m, 1H), 1.35 (m, 2H), 1.26 (s, 6H), 0.89 (d, $J=6.6$ Hz, 3H), 0.88 (d, $J=6.8$ Hz, 3H); ^{13}C NMR (125 MHz, CD_3OD): δ 175.97 (s), 174.68 (s), 173.34 (s), 173.04 (s), 158.51 (s), 157.97 (s), 154.71 (s), 150.98 (s), 143.63 (s×3), 139.64 (d), 137.98 (s), 137.68 (s), 136.76 (s), 136.54 (s), 136.08 (s), 134.93 (s), 131.68 (s), 130.90 (d×6), 129.46 (d×2), 129.30 (d×3), 129.26 (d×6), 128.99 (d), 128.85 (d×2), 125.46 (d×2), 124.93 (s), 123.68 (d), 121.28 (d), 120.12 (d), 119.32 (s), 117.24 (s), 116.11 (d), 84.81 (s), 76.86 (s), 74.82 (s), 67.82 (t), 59.93 (d), 56.20 (d), 55.30 (d), 54.86 (d), 41.33 (t), 33.77 (t), 31.72 (d), 31.13 (t), 30.04 (t), 28.47 (q×3), 28.15 (t), 26.98 (q×2), 26.62 (t), 22.37 (t), 19.80 (q), 19.03 (q), 18.36 (q), 17.96 (q), 12.35 (q); anal. calcd for $C_{74}H_{87}N_{11}O_{11}S$: C 66.40, H 6.55, N 11.51; found: C 65.42, H 6.66, N 11.23; MS (ESI, MeOH): *m/z* (%) 1339 (100) M^+, 1361 (10) $M+Na^+$.

4.7. H-Arg(Pmc)-Trp(Boc)-His(Trt)-Val-NH_2 (general procedure C)

$Pd(OH)_2/C$ (5 mg) was added to a solution of *Z*-Arg(Pmc)-Trp(Boc)-His(Trt)-Val-NH_2 (155 mg, 0.116 mmol) in MeOH (6 mL). The suspension was degassed and set under H_2-atmosphere. After stirring for 4 h at rt, the reaction mixture was filtered through Celite, and the filtrate was concentrated in vacuo. Column chromatography (CH_2Cl_2/MeOH 10:1, $R_f=0.3$; first with 10:1, then to 6.7:1) of the crude product yielded pure H-Arg(Pmc)-Trp(Boc)-His(Trt)-Val-NH_2 (113 mg, 81%) as colorless solid. α_D^{20} −1.20 (*c* 1.00, MeOH); mp: 136.0–136.5 °C; IR (film) ν 3419 (m), 3316 (m), 1728 (s), 1654 (s), 1545 (s) cm^{-1}; ^1H NMR (500 MHz, CD_3OD): δ 8.03 (br. d, $J=8.2$ Hz, 1H), 7.57 (d, $J=7.8$ Hz, 1H), 7.50 (s, 1H), 7.34–7.27 (m, 10H), 7.22 (m, 1H), 7.16 (m, 1H), 7.09–7.07 (m, 6H), 6.79 (s, 1H), 4.68 (dd, $J=10.0$, 4.5 Hz, 1H), 4.66 (dd, $J=7.7$, 5.6 Hz, 1H), 4.19 (d, $J=5.2$ Hz, 1H), 3.20 (m, 1H), 3.17 (m, 1H), 3.02–2.95 (m, 4H), 2.89 (dd, $J=14.8$, 7.7 Hz, 1H), 2.58 (t, $J=6.8$ Hz, 2H), 2.53 (s, 3H), 2.51 (s, 3H), 2.11–2.05 (m, 1H), 2.05 (s, 3H), 1.75 (t, $J=6.8$ Hz, 2H), 1.62 (s, 9H), 1.49–1.46 (m, 1H), 1.34–1.25 (m, 3H), 1.25 (s, 6H), 0.89 (d, $J=6.6$ Hz, 3H), 0.88 (d, $J=6.6$ Hz, 3H); ^{13}C NMR (125 MHz, CD_3OD): δ 177.74 (s), 175.95 (s), 173.37 (s), 173.07 (s), 157.97 (s), 154.71 (s), 150.98 (s), 143.67 (s×3), 139.67 (d), 137.56 (s), 136.77 (s), 136.56 (s), 136.07 (s), 134.93 (s), 131.78 (s), 130.93 (d×6), 129.34 (d×3), 129.29 (d×6), 125.55 (d), 125.43 (d), 124.96 (s), 123.69 (d), 121.32 (d), 120.23 (d), 119.34 (s), 117.38 (s), 116.19 (d), 84.93 (s), 76.87 (s), 74.86 (s), 59.87 (d), 55.55 (d), 55.00 (d), 54.68 (d), 41.58 (t), 33.81 (t), 33.00 (t), 31.80 (d), 31.26 (t), 28.55 (t), 28.52 (q×3), 27.04 (t×2), 26.42 (t), 22.40 (t), 19.86 (q), 19.08 (q), 18.39 (q), 17.99 (q), 12.41 (q); anal. calcd for $C_{66}H_{81}N_{11}O_9S$: C 65.81, H 6.78, N 12.79; found: C 64.05, H 6.76, N 12.38; MS (ESI, MeOH): *m/z* (%) 1205 (100) $M+H^+$, 1227 (16) $M+Na^+$.

4.8. *Z*-Leu-Arg(Pmc)-Trp(Boc)-His(Trt)-Val-NH_2

Coupling of H-Arg(Pmc)-Trp(Boc)-His(Trt)-Val-NH_2 (97 mg, 0.08 mmol) with *Z*-Leu-OH (25.6 mg, 0.10 mmol) following the procedure A and purification of the crude product by column chromatography (CH_2Cl_2/MeOH 10:1, $R_f=0.5$; with 15:1) yielded HPLC-pure (YMC-Pack SIL, 50×4 mm, CH_2Cl_2/MeOH 95:05, 1 mL/min, $R_t=1.62$ min) *Z*-Leu-Arg(Pmc)-Trp(Boc)-His(Trt)-Val-NH_2 (106 mg, 91%) as colorless solid. α_D^{20} −3.10 (*c* 1.00, MeOH); mp: 142.0–142.5 °C; IR (film) ν 3440 (m), 3311 (m), 1728 (s), 1650 (s), 1535 (s) cm^{-1}; ^1H NMR (500 MHz, CD_3OD): δ 8.00 (br. d, $J=8.2$ Hz, 1H), 7.45 (d, $J=7.9$ Hz, 1H), 7.46 (s, 1H), 7.35 (s, 1H), 7.35–7.25 (m, 9H), 7.27–7.23 (m, 3H), 7.22 (m, 1H), 7.17–7.14 (m, 2H), 7.15 (m, 1H), 7.08 (m, 6H), 6.84 (s, 1H), 4.81 (d, $J=12.9$ Hz, 1H), 4.78 (d, $J=12.9$ Hz, 1H), 4.62 (dd, $J=7.9$, 5.7 Hz, 1H), 4.58 (dd, $J=9.5$, 4.8 Hz, 1H), 4.23 (dd, $J=7.9$, 5.4 Hz, 1H), 4.17 (d, $J=6.3$ Hz, 1H), 3.88 (br. t, $J=7.6$ Hz, 1H), 3.20–3.13 (m, 2H), 3.03-2.98 (m, 4H), 2.60 (t, $J=6.9$ Hz, 2H), 2.53 (s, 3H), 2.51 (s, 3H), 2.12 (m, 1H), 2.06 (s, 3H), 1.78 (t, $J=6.9$ Hz, 2H), 1.72–1.69 (m, 1H), 1.61–1.57 (m, 2H), 1.60 (s, 9H), 1.44–1.42 (m, 4H), 1.27 (s, 6H), 0.90 (d, $J=6.7$ Hz, 3H), 0.89 (d, $J=6.7$ Hz, 3H), 0.85 (d, $J=6.4$ Hz, 3H), 0.83 (d, $J=6.7$ Hz, 3H); ^{13}C NMR (125 MHz, CD_3OD): δ 179.15 (s), 174.64 (s), 172.92 (s), 172.20 (s), 171.80 (s), 157.32 (s), 156.61 (s), 153.33 (s), 149.63 (s), 142.29 (s×3), 138.25 (s), 138.25 (d), 136.39 (s×2), 135.15 (s), 134.69 (s), 133.40 (s), 130.25 (s), 129.51 (d×6), 128.03 (d×2), 127.92 (d×3), 127.89 (d×6), 127.61 (d), 127.27 (d×2), 124.16 (d), 123.67 (d), 123.54 (s), 122.31 (d), 119.78 (d), 118.72 (d), 117.93 (s), 116.06 (s), 114.80 (d), 83.54 (s), 75.45 (s), 73.45 (s), 66.38 (t), 58.71 (d), 54.24 (d), 54.03 (d), 53.87 (d), 53.52 (d), 40.20 (t), 39.73 (t), 32.39 (t), 30.25 (d), 29.85 (t), 28.22 (t), 27.09 (q×3), 26.73 (t), 25.58 (q×2), 25.11 (t), 24.43 (t), 21.86 (q), 20.99 (t), 20.90 (q), 18.40 (q), 17.64 (q), 17.06 (q), 16.56 (q), 10.95 (q); anal. calcd for $C_{80}H_{98}N_{12}O_{12}S$: C 66.19, H 6.80, N 11.58; found: C 63.78, H 6.87, N 10.87; MS (ESI, MeOH): *m/z* (%) 1453 (100) $M+H^+$, 1475 (91) $M+Na^+$.

4.9. H-Leu-Arg(Pmc)-Trp(Boc)-His(Trt)-Val-NH_2 (7b)

Deprotection of *Z*-Leu-Arg(Pmc)-Trp(Boc)-His(Trt)-Val-NH_2 (200 mg, 0.138 mmol) following the procedure C and purification of the crude product by column chromatography (CH_2Cl_2/MeOH 10:1, $R_f=0.5$; first with 20:1, then to 6:1) furnished HPLC-pure (YMC-Pack SIL, 50×4 mm, CH_2Cl_2/MeOH 90:10, 1 mL/min, $R_t=1.89$ min) **7b** (132.9 mg, 73%) as a colorless solid. α_D^{20} −3.74 (*c* 1.00, MeOH); mp: 137.0–137.5 °C; IR (film) ν 3343 (m), 3311 (m), 1722 (s), 1644 (s), 1539 (s) cm^{-1}; ^1H NMR (500 MHz, CD_3OD): δ 8.03 (br. d, $J=7.9$ Hz, 1H), 7.54 (d, $J=7.6$ Hz, 1H), 7.49 (s, 1H), 7.35 (d, $J=1.3$ Hz, 1H), 7.33–7.26 (m, 9H), 7.23 (ddd, $J=8.2$, 7.2, 1.0 Hz, 1H), 7.16 (m, 1H), 7.09–7.07 (m,

6H), 6.81 (s, 1H), 4.66–4.62 (m, 2H), 4.35 (dd, $J=7.0$, 6.0 Hz, 1H), 4.18 (d, $J=4.8$ Hz, 1H), 3.27 (dd, $J=8.9$, 5.4 Hz, 1H), 3.15 (dd, $J=14.9$, 4.5 Hz, 1H), 3.15 (m, 1H), 3.02–2.96 (m, 3H), 2.91 (dd, $J=14.5$, 8.2 Hz, 1H), 2.62 (t, $J=7.0$ Hz, 2H), 2.54 (s, 3H), 2.52 (s, 3H), 2.12–2.07 (m, 1H), 2.06 (s, 3H), 1.78 (t, $J=7.0$ Hz, 2H), 1.74–1.67 (m, 1H), 1.64–1.50 (m, 2H), 1.61 (s, 9H), 1.45-1.36 (m, 3H), 1.27 (s, 6H), 1.25–1.20 (m, 1H), 0.90 (d, $J=6.6$ Hz, 3H), 0.89 (d, $J=7.0$ Hz, 3H), 0.84 (d, $J=6.6$ Hz, 3H), 0.81 (d, $J=6.6$ Hz, 3H); ^{13}C NMR (125 MHz, CD_3OD): δ 178.36 (s), 176.38 (s), 174.35 (s), 173.65 (s), 173.50 (s), 158.44 (s), 155.13 (s), 151.43 (s), 144.07 (s×3), 140.08 (d), 138.00 (s), 137.15 (s), 136.98 (s), 136.51 (s), 135.22 (s), 132.11 (s), 131.33 (d×6), 129.72 (d×3), 129.69 (d×6), 125.94 (d), 125.86 (d), 125.36 (s), 124.08 (d), 121.74 (d), 120.58 (d), 119.73 (s), 117.56 (s), 116.55 (d), 85.26 (s), 77.26 (s), 75.26 (s), 60.34 (d), 55.49 (d), 55.40 (d), 54.79 (d), 54.22 (d), 45.68 (t), 41.68 (t), 34.21 (t), 32.18 (d), 31.71 (t), 30.69 (t), 28.93 (q×3), 28.89 (t), 27.42 (q×2), 27.08 (t), 26.15 (t), 24.01 (q), 22.82 (t), 22.68 (q), 20.24 (q), 19.50 (q), 18.79 (q), 18.41 (q), 12.79 (q); anal. calcd for $C_{72}H_{92}N_{12}O_{10}S$: C 65.63, H 7.04, N 12.76; found: C 64.29, H 7.19, N 12.38; MS (ESI, MeOH): m/z (%) 1318 (100) $M+H^+$, 1340 (95) $M+Na^+$.

4.10. $1^3,2^3,3^2,4^3,5^2,6^3,7^2,8^3$-Octakis(*Gla*-Leu-Arg(Pmc)-Trp(Boc)-His(Trt)-Val-NH_2)-*p*-octiphenyl (7c)

H-Leu-Arg(Pmc)-Trp(Boc)-His(Trt)-Val-NH_2 (**7b**) (83.6 mg, 63.4 μmol), HBTU (57 mg, 150 μmol) and Et_3N (21.3 μL, 153 μmol) were added to a solution of *p*-octiphenyl (**7a**) (5.09 mg, 4.23 μmol) in DMF (1 mL) and stirred for 3 h at rt with occasional sonication. The reaction mixture was dried in vacuo. Purification of the crude product by PTLC ($CHCl_3$/MeOH 5:1, $R_f=0.6$), then again by PTLC ($CHCl_3$/MeOH 4:1, $R_f=0.8$) yielded **7c** (27.4 mg, 56%) as colorless solid. Purity of the product was verified using HPLC (YMC-Pack SIL 50×4 mm, CH_2Cl_2–MeOH 92:08, 1 mL/min, $R_t=0.74$ min). ^{1}H NMR (300 MHz, CD_3OD): δ 8.05–7.90 (m, 8H), 7.53-6.90 (m, 186H), 6.78 (s, 2H), 6.70 (s, 6H), 4.85–4.06 (several m, 56H), 3.20–2.80 (m, 48H), 2.60–2.40 (m, 64H), 2.16–1.99 (m, 8H), 2.04 (s, 8H), 2.00 (s, 16H), 1.80–1.14 (several m, 72H), 1.60 (s, 18H), 1.55 (s, 18H), 1.51 (s, 36H), 1.25 (s, 12H), 1.24 (s, 12H), 1.22 (s, 24H), 1.80-1.14 (several m, 192H), 0.90–0.50 (m, 96H); MS (ESI, CH_2Cl_2/CH_3CN/H_2O/MeOH/AcOH 40:37:12:10:1): m/z (%) 1451 (41) $M+8H^{8+}$, 1658 (100) $M+7H^{7+}$, 1934 (79) $M+6H^{6+}$, 2321 (40) $M+5H^{5+}$.

4.11. $1^3,2^3,3^2,4^3,5^2,6^3,7^2,8^3$-Octakis(*Gla*-Leu-Arg-Trp-His-Val-NH_2)-*p*-octiphenyl = 1,1,1″,1‴,1⁗,1⁗′,1⁗″,1⁗‴-{[1,1′:4′,1″:4″,1‴:4‴,1⁗:4⁗,1⁗′:4⁗′,1⁗″:4⁗″,1⁗‴:4⁗‴,1⁗⁗:4⁗⁗-octiphenyl]-2″,2‴,2⁗′,2⁗″,3,3′,3‴,3⁗′,3⁗″,3⁗‴-octaoyloctakis[oxy(1-oxoethane-2,1-diyl)]}octakis[L-leucyl-L-arginyl-L-tryptophanyl-L-histidyl-L-valinamide] (7)

A solution of **7c** (10.5 mg, 0.91 μmol) in TFA (2 mL) was stirred for 1 h at rt. After addition of CH_2Cl_2 (2 mL) and evaporation of the solvent, the crude solid was washed with hexane (500 μL, 4×) and CH_2Cl_2 (500 μL, 2×), redissolved in TFA (2 mL), stirred for 1 h at rt, diluted with CH_2Cl_2 (2 mL), evaporated, dried in vacuo, azeotroped with toluene (500 μL, 3×), washed with Et_2O (500 μL, 4×), hexane (500 μL, 4×) and CH_2Cl_2 (500 μL, 2×) to give RP-HPLC-pure (YMC-Pack ODS-A, 250×10 mm, MeOH (1% TFA)/H_2O 78:22, 2 mL/min, $R_t=5.30$ min) **7** [3.2 mg, 53% (calcd from UV)] as a colorless solid. ^{1}H NMR (300 MHz, CD_3OD–CF_3COOD 1:1): δ 8.69–8.61 (m, 8H), 7.48–6.97 (m, 74H), 4.72 (m, 32H), 4.36 (m, 16H), 3.99 (m, 8H), 3.56–3.09 (m, 48H), 2.20–2.00 (m, 8H), 2.00–1.14 (m, 64H), 1.12–0.56 (m, 96H); MS (MALDI-TOF; sinapic acid matrix): m/z 6730.6 $M+H^+$.

4.12. BLM recordings

Experimental setup for BLM conductance measurements was as described in ref 28. BLMs were formed by painting a solution of EYPC in *n*-decane (42 mg/mL) on an aperture (d = 150 μm) in a delrin cuvette. Periodical check of overall performance of the employed system was done with alamethicin.

Conditions for single- and multichannel experiments with identical *cis* and *trans* chambers: (a) 1.3 M KCl, 5 mM MES, pH = 5.0,[28] (b) 1.0 M KCl, 10 mM NaOAc, pH = 4.0–5.6, (b) 1.0 M KCl, 10 mM MES, pH = 6.0. Cation **7** (100 nM) was added *cis* at $V=+50$ mV, anion HPTS (0–200 μM) was added *trans* at $V=+50$ mV. Conditions for multichannel ion selectivity experiments with different *cis* and *trans* chambers: 1.0 M KCl in *cis*, 0.1 M KCl in *trans*, 10 mM NaOAc (pH < 5.6) or 10 mM MES (pH > 5.6) in both chambers.

Permeability ratios were calculated from experimentally determined reversal potentials V_r under asymmetric conditions using the equation derived from Goldman–Hodgkin–Katz equation,[42] and plotted as a function of pH (Fig. 2).

Dissociation constants were calculated using eq. 2:

$$\log(Y/(1-Y)) = n\log[\text{guest}] - n\log K_D \quad (2)$$

where Y is the fractional saturation $[(I^{max}-I)/(I^{max}-I^{min})]$, n the Hill coefficient, and K_D the dissociation constant.

4.13. EYPC-LUVs⊃ANTS/DPX

The following buffers were used: Buffer A, 12.5 mM ANTS, 45.0 mM DPX, 5 mM TES, 20 mM KCl, pH = 7.0; buffer B, 5 mM TES, 100 mM KCl, pH = 7.0; buffer C, 10 mM MES, 100 mM KCl, pH 4.5∼7.0. A thin film of EYPC (25 mg) was prepared by evaporating a solution of EYPC in $CHCl_3$ and MeOH (1 mL each) on a rotary evaporator and then in vacuo (>2 h), and then hydrated with 1 mL buffer A (>30 min). The resulting suspension was subjected to >5 freeze-thaw cycles (using liquid N_2 to freeze and a warm water bath to thaw), and >10 times extruded using a Mini-Extruder through a 100 nm polycarbonate membrane

(Avanti).[33] External ANTS/DPX was removed by gel filtration (Sephadex G-50) using buffer B and diluted with the same buffer to 6 mL to give EYPC-LUVs⊃ANTS/DPX stock solution (5 mM PC).

4.14. ANTS/DPX-assay[24–26]

Above EYPC-LUVs⊃ANTS/DPX (100 μL) were added to gently stirred, thermostated buffer C (1.90 mL, 10 mM MES, 100 mM KCl, pH = 4.5∼7.0) in a fluorescence cuvette. Fluorescence emission intensity I_t ($\lambda_{em} = 510$ nm, $\lambda_{ex} = 353$ nm) was monitored as a function of time (t) during addition of barrel **6** or **7** (c_M 0–250 nM) and 40 μL 1.2% aq triton X-100. Flux curves were normalized to fractional activity Y using equation:

$$Y = (I_t - I_0)/(I_\infty - I_0)$$

in which I_0, is I_t right before the addition of the samples and I_∞ is I_t after addition of triton X-100.

4.15. Fluorescence depth quenching[23,21,46,47]

5-/12-DOXYL labeled EYPC LUVs were prepared similarly by extrusion method. A solution of 5- (or 12-) DOXYL-PC (2 mg) and EYPC (18 mg) in $CHCl_3$ and MeOH (0.5 mL each) was dried to give a thin film, which was hydrated with buffer B (400 μL, >30 min). After >5 freeze–thaw cycles, the suspension was passed through a polycarbonate film (100 nm pore size, 15 times), and used without further purification. The stock solution of thus prepared 5-(or 12-)DOXYL-PC (8.3 μL) was diluted with buffer C (2 mL) and the sample (**7**, c_M 200 nM) was added. Fluorescence emission spectra were recorded with λ_{ex} at 320 nm.

4.16. Abbreviations and symbols

ANTS, 8-aminonaphthalene-1,3,6-trisulfonic acid, disodium salt; BLM, black (planar) lipid membrane; Boc, *tert*-butoxycarbonyl; c_M, concentration of monomer used; $c_{M,Y<0.5}$, c_M which gives $Y < 0.5$; CR, central; DOXYL, 4,4-dimethyl-3-oxazolidinyloxy; 5- (or 12-) DOXYL-PC, 1-palmitoyl-2-stearoyl-(5- (or 12-)DOXYL)-*sn*-glycero-3-phosphocholine; DPX, *p*-xylene-bis-pyridinium bromide; EDC, 1-(3-dimethylaminopropyl)-3-ethyl-carbodiimide; Fmoc, fluorenylmethoxycarbonyl; HBTU, O-benzotriazolyl-*N*,*N*,*N*′,*N*′-tetramethyluronium hexafluorophosphate; HOBt, 1-hydroxybenzotriazole; HPTS, 8-hydroxypyrene-1,3,6-trisulfonic acid, trisodium salt; Pmc, 2,2,5,7,8-pentamethylchroman-6-sulfonyl; TEA, triethylamine; TFA, trifluoroacetic acid; Trt, trityl; Y, fractional activity; Z, benzyloxycarbonyl.

Acknowledgements

We thank D. Jeannerat, A. Pinto, and J.-P. Saulnier for NMR measurements, H. Eder for elemental analyses, the group of F. Gülaçar for MS measurements, R. E. Offord for assistance with MALDI-TOF, one referee for helpful comments, and the Swiss NSF for financial support (2000-064818.01 and National Research Program 'Supramolecular Functional Materials' 4047-057496).

References and notes

1. Matile, S. *Chem. Soc. Rev.* **2001**, *30*, 158.
2. Matile, S. *Chem. Rec.* **2001**, *1*, 162.
3. Baudry, Y.; Baumeister, B.; Das, G.; Gerard, D.; Matile, S.; Sakai, N.; Som, A.; Sordé, N.; Talukdar, P. *Chimia* **2002**, *56*, 667.
4. Scrimin, P.; Tecilla, P. *Curr. Opin. Chem. Biol.* **1999**, *3*, 730.
5. Gokel, G. W.; Mukhopadhyay, A. *Chem. Soc. Rev.* **2001**, *30*, 274.
6. Kirkovits, G. J.; Hall, C. D. *Adv. Supramol. Chem.* **2000**, *7*, 1.
7. Sidorov, V.; Kotch, F. W.; Abdrakhmanova, G.; Mizani, R.; Fettinger, J. C.; Davis, J. T. *J. Am. Chem. Soc.* **2002**, *124*, 2267.
8. Bandyopadhyay, P.; Bandyopadhyay, P.; Regen, S. L. *J. Am. Chem. Soc.* **2002**, *124*, 11254.
9. Cameron, L. M.; Fyles, T. M.; Hu, C. W. *J. Org. Chem.* **2002**, *67*, 1548.
10. Wright, A. J.; Matthews, S. E.; Fischer, W. B.; Beer, P. D. *Chem. Eur. J.* **2001**, *7*, 3474.
11. Das, S.; Seebach, D.; Reusch, R. N. *Biochemistry* **2002**, *41*, 5307.
12. Goto, C.; Yamamura, M.; Satake, A.; Kobuke, Y. *J. Am. Chem. Soc.* **2001**, *123*, 12152.
13. Arndt, H.-D.; Knoll, A.; Koert, U. *Angew. Chem., Int. Ed.* **2001**, *40*, 2076.
14. Vandenburg, Y. R.; Smith, B. D.; Biron, E.; Voyer, N. *Chem. Commun.* **2002**, 694.
15. Carrasco, H.; Foces-Foces, C.; Perez, C.; Rodriguez, M. L.; Martin, J. D. *J. Am. Chem. Soc.* **2001**, *123*, 11970.
16. Arnt, L.; Tew, G. N. *J. Am. Chem. Soc.* **2002**, *124*, 7664.
17. Sanchez-Quesada, J.; Isler, M. P.; Ghadiri, M. R. *J. Am. Chem. Soc.* **2002**, *124*, 10004.
18. Wang, D.; Guo, L.; Zhang, J.; Jones, L. R.; Chen, Z.; Pritchard, C.; Roeske, R. W. C. *J. Pept. Res.* **2001**, *57*, 301.
19. Sanderson, J. M.; Yazdani, S. *Chem. Commun.* **2002**, 1154.
20. Sakai, N.; Matile, S. *J. Am. Chem. Soc.* **2002**, *124*, 1184.
21. Baumeister, B.; Sakai, N.; Matile, S. *Angew. Chem., Int. Ed.* **2000**, *39*, 1955.
22. Sakai, N.; Baumeister, B.; Matile, S. *ChemBioChem.* **2000**, *1*, 123.
23. Sakai, N.; Houdebert, D.; Matile, S. *Chem. Eur. J.* **2003**, *9*, 223.
24. Baumeister, B.; Som, A.; Das, G.; Sakai, N.; Vilbois, F.; Gerard, D.; Shahi, S. P.; Matile, S. *Helv. Chim. Acta* **2002**, *85*, 2740.
25. Das, G.; Matile, S. *Proc. Natl. Acad. Sci. U.S.A.* **2002**, *99*, 5183.
26. Das, G.; Onouchi, H.; Yashima, E.; Sakai, N.; Matile, S. *ChemBioChem.* **2002**, *3*, 1089.
27. Das, G.; Talukdar, P.; Matile, S. *Science* **2002**, *298*, 1600.
28. Baumeister, B.; Sakai, N.; Matile, S. *Org. Lett.* **2001**, *3*, 4229.
29. Som, A.; Sakai, N.; Matile, S. *Bioorg. Med. Chem.* **2003**, *11*, 1363.
30. Som, A.; Matile, S. *Eur. J. Org. Chem.* **2002**, 3874.
31. Baumeister, B.; Matile, S. *Macromolecules* **2002**, *35*, 1549.

32. Das, G.; Ouali, L.; Adrian, M.; Baumeister, B.; Wilkinson, K. J.; Matile, S. *Angew. Chem., Int. Ed.* **2001**, *40*, 4657.
33. Sordé, N.; Matile, S. *J. Supramol. Chem.* **2002**, *2*, 191.
34. Sakai, N.; Sordé, N.; Das, G.; Perrottet, P.; Gerard, D.; Matile, S. *Org. Biomol. Chem.* **2003**, *1*, 1226.
35. Sakai, N.; Majumdar, N.; Matile, S. *J. Am. Chem. Soc.* **1999**, *121*, 4294.
36. Wimley, W. C.; White, S. H. *Nature Struct. Biol.* **1996**, *3*, 842.
37. Sazaki, T.; Lieberman, M. Protein Mimetics. In *Comprehensive Supramolecular Chemistry, Vol. 4*; Murakami, Y., Ed.; Elsevier: Oxford, 1996; p 193–243.
38. Yau, W.-M.; Wimley, W. C.; Gawrisch, K.; White, S. H. *Biochemistry* **1998**, *37*, 14713.
39. Ridder, A. N. J. A.; Morein, S.; Stam, J. G.; Kuhn, A.; de Kruijff, B.; Killian, J. A. *Biochemistry* **2000**, *39*, 6521.
40. De Planque, M. R. R.; Kruijtzer, J. A. W.; Liskamp, R. M. J.; Marsh, D.; Greathouse, D. V.; Koeppe, R. E., II; de Kruijff, B.; Killian, J. A. *J. Biol. Chem.* **1999**, *274*, 20839.
41. Sakai, N.; Sordé, N.; Matile, S. *J. Am. Chem. Soc.* **2003**, *125*, 7776.
42. Hille, B. *Ionic Channels of Excitable Membranes*; Sinauer: Sunderland, MA, 1992.
43. Matsuzaki, K.; Murase, O.; Fujii, N.; Miyajima, K. *Biochemistry* **1996**, *35*, 11361.
44. Yang, L.; Harroun, T. A.; Weiss, T. M.; Ding, L.; Huang, H. W. *Biophys. J.* **2001**, *81*, 1475.
45. Zasloff, M. *Nature* **2002**, *415*, 389.
46. Sakai, N.; Matile, S. *Chem. Eur. J.* **2000**, *6*, 1731.
47. Ni, C.; Matile, S. *Chem. Commun.* **1998**, 755.
48. Stankowski, S.; Pawlak, M.; Kaisheva, E.; Robert, C. H.; Schwarz, G. *Biochim. Biophys. Acta* **1991**, *1069*, 77.
49. Schmidtchen, F. P.; Berger, M. *Chem. Rev.* **1997**, *97*, 1609.